International Conference on Fluid Dynamics and Thermodynamics, Dubai, January 25-27,2011

Investigation of Turbulence Model to Simulation of Ground Effect in 2D and 3D Cases

M. H. Djavareshkian, A.Parsania, A.Esmaeli, and A. Ziaforoghi

Abstract— The aim of the present study is to investigate the effect of turbulence models on the 2D and 3D simulation of the wing in the ground effect. A pressure-based is the procedure to solving Navier Stokes equations on a nonorthogonal mesh with collocated finite volume formulation for incompressible flows. The procedure incorporates several eddy-viscosity turbulence models for simulation of the ground effect. In this study 3D simulation around the wing with airfoil-NACA 6409 section are compared with experimental data. Also in 2D simulation the flow around NACA0015 airfoil has been investigated for different turbulence models. The RANS turbulence models is used in this research for 2D and 3D cases and various aerodynamic parameters has been studied in the different ground clearances and angle of attacks. Computation visualization of the flows shows that the turbulent models have more effect on the simulation in the small ground clearance. The result shows that Spalart-Allmarast is interested for 2D and 3D cases because of its simplification and its good agreement with experimental results.

Keywords— Ground effect, Turbulence model, 2D, 3D, NACA0015, NACA 6409.

I. INTRODUCTION

An enhancement of lift for airfoils in proximity to the ground surface is called a wing in ground (WIG) effect. Wing-in-ground-effect (WIG) vehicles are expected to become one of high speed and efficient transportation systems. When a wing is going near the surface the mass flow under the airfoil is decreased, pressure begins to build on the lower surface of the wing and air cushion is created by the high pressure that buildup under it. Also the induced downwash velocity diminishes close to the ground and induced drag for a wing is lowered and the effective angle of attack increases. Both of these occurrences result in an overall increase in the L/D ratio of the airfoil.

In recent years, there have been successful investigations on the aerodynamics of airfoil and wing. One of the more recent wind tunnel experiments was done by Ahmed et al. [1], [2]. They investigated effect of variation of AOA and ground clearance on aerodynamic characteristics of symmetrical airfoil NACA 0015 and NACA 4412 airfoil in ground effect.

Kawazoe et al. [3] conduct their study on dynamic characteristics of delta wing in rolling motion near ground. Water tunnel investigation of Pairs of Vortex Filaments in Ground Effect has been done by Kliment et al.[4]. Zhang et al. [5] tested the aerodynamic behavior of a cambered, double element, high-lift wing in ground proximate in wind tunnel. Aerodynamic Ground Effects of a Tailless Chevron-Shaped UCAV Model were investigated by Jones et al. [6] in wind tunnel. Ogurek et al. [7] investigate various sizes of winglet designs for a wing both in and out of ground effect. The experiment results showed that using winglet has greater advantage both in and out of ground effect. The aerodynamic characteristics of NACA6409 in ground proximity tested by Jung et al. [8]. They investigated the influence of Aspect ratio of wing, endplate and the shape of it in different angle of attack and ground clearance.

Smith [9] performed the computational analysis of airfoils in ground effect. Patrick Vu [10] studied wing tip vortices in inverted airfoils close to the ground for use in racing car. Influence of endplate on aerodynamic characteristics for low-aspect-ratio wing in ground effect is performed by Park et al. [11]. Abramowski [12] presents numerical Investigation of NACA/Munk M15 airfoil in ground proximity. Moon et al. [13] simulated three-dimensional wings in ground effect for aero-levitation electric vehicle. Angle et al.[14] focused their research on Pitch Stability Analysis of an Airfoil in Ground Effect. Aeronumeric optimal design of a wing in-ground-effect craft performed by Kim et al. [15]. In this research determination of the planform configuration, the aspect ratio, and the position of the tail wing within the design constraints were performed. Effect of ground proximity on the aerodynamic performance and stability of a light unmanned aerial vehicle has been performed by Boschetti and et al. [16]. The shape optimization using the multi-objective genetic algorithm and the analysis of the 3-dimensional wings in ground effect has been performed by Lee and et al can be seen in ref [17].

In all of above research the effect of turbulence models has not been compared in 2D and 3D cases. In this research, the effect of turbulence models has been studied in different AOA

M. H. Djavareshkian is with the Department of Mechanical Engineering, Ferdowsi University of Mashhad, Mashhad, Iran; e-mail: javareshkian@ferdowsi.um.ac.ir.

A.Parsania was with Department of Mechanical Engineering, Ferdowsi University of Mashhad, Mashhad, Iran; e-mail: ahmad.parssnia@gmail.com.

A.Esmaeli is with the Department of Mechanical Engineering, Ferdowsi University of Mashhad, Mashhad, Iran; e-mail: aliesmaeli@gmail.com.

A. Ziaforoghi is with the Department of Mechanical Engineering, Ferdowsi University of Mashhad, Mashhad, Iran; e-mail: amin.zia.f@gmail.com.

an different distance from the ground (ground clearance) for both 2D and 3D cases and results has been presented.

TABLE I
UNITS FOR MAGNETIC PROPERTIES

Symbol	Quantity
A	Cell Face Area
AOA	angle of attack
C	Cord Length
CD	Drag Coefficient
CL	Lift Coefficient
CFD	Computation Fluid Dynamic
D	Drag Force
2D	Two Dimensional
3D	Three Dimensional
h	Ground Clearances
I	Flux
L	Lift Force
P	Pressure
$\vec{\mathbf{q}}$	Scalar Flux Vector
Re	Reynolds Number
$\vec{S}$	Source Term
SA	Spalart Allmaras Model
$\vec{\mathbf{T}}$	Stress Tensor
$\vec{\mathbf{V}}$	Velocity Vector
WIG	Wing in Ground Effect
ϕ	Scalar Quantity
ρ	Density
μ	Dynamic Viscosity
Γ	Diffusivity Coefficient

II. GOVERNING EQUATION FOR FLUID

The basic equations, which describe conservation of mass, momentum and scalar quantities, can be expressed in the following vector form, which is independent of used coordinate system.

$$\frac{\partial \rho}{\partial t} + div(\rho \vec{\mathbf{V}}) = S_m \qquad (1)$$

$$\frac{\partial(\rho\vec{\mathbf{V}})}{\partial t} + div(\rho\vec{\mathbf{V}}\otimes\vec{\mathbf{V}} - \vec{\mathbf{T}}) = \vec{\mathbf{S}}_{\mathbf{v}} \qquad (2)$$

$$\frac{\partial(\rho\phi)}{\partial t} + div(\rho\vec{\mathbf{V}}\phi - \vec{\mathbf{q}}) = \vec{\mathbf{S}}_{\mathbf{\Phi}} \qquad (3)$$

Where ρ , $\vec{\mathbf{V}}$ and ϕ are density, velocity vector and scalar quantity respectively, $\vec{\mathbf{T}}$ is the stress tensor and $\vec{\mathbf{q}}$ is the scalar flux vector. The latter two are usually expressed in terms of basic dependent variables. The stress tensor for a Newtonian fluid is:

$$\vec{\mathbf{T}} = -(\mathrm{P} + \frac{2}{3}\mu \ \mathrm{div}\ \vec{\mathbf{V}})\vec{\mathbf{I}} + 2\mu\vec{\mathbf{D}} \qquad (4)$$

And the Fourier-type law usually gives the scalar flux vector:

$$\vec{\mathbf{q}} = \Gamma_\phi \ \mathrm{grad}\Phi \qquad (5)$$

For the purpose of illustration (3) may be expressed in 2D Cartesian coordinates as:

$$\overbrace{\frac{\partial(\rho\phi)}{\partial t}}^{\text{transient term}} + \overbrace{\frac{\partial(\rho u\phi)}{\partial x} + \frac{\partial(\rho v\phi)}{\partial y}}^{\text{convection term}} \overbrace{- \frac{\partial}{\partial x}(\Gamma_\phi\frac{\partial\phi}{\partial x}) - \frac{\partial}{\partial y}(\Gamma_\phi\frac{\partial\phi}{\partial y})}^{\text{diffusion term}} = \overbrace{S_\phi}^{\text{source}} \qquad (6)$$

Integration of (6) over a finite volume (see e.g. Figure. 1) and application of the Gauss divergence Theorem yield a balance involving the rate of change in ϕ, face fluxes and volume-integrated net source. The discretized equations resulting according to SIMPLE algorithm take the form:

$$A_P.\phi_P = \sum_{m=E,W,N,S} A_m.\phi_m + S'_\phi \qquad (7)$$

Where A's are the convection-diffusion coefficients. The term S'_ϕ in Eq. (7) contains quantities arising from non-orthogonality, numerical dissipation terms, external sources, deferred correction terms, and $(\rho\delta\upsilon/\delta t)\phi_P$ of the old time-step/iteration level. For the momentum equations it is easy to separate out the pressure-gradient source from the convected momentum fluxes.

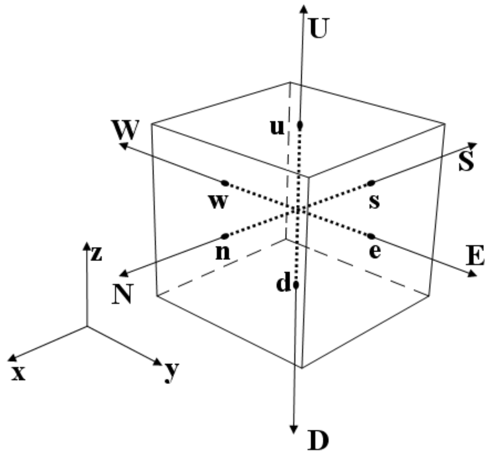

Fig. 1 Finite volume and storage arrangement

III. RESULTS AND DISCUSSES

The results are presented and discussed in this section. In this paper the main emphasis is concentrated on the simulation of incompressible flow around the airfoil and a wing close to the ground. Computational results are shown in followed figures for a baseline series of test cases.

A. The 2D simulations condition

Simulation of flow around the airfoil NACA0015 has been performed. The simulation is two-dimensional, steady stat and incompressible. The Reynolds number is 2.4×10^5 .

The grid structure that used in 2D CFD simulation was created by H mesh (see e.g. Figure.2). Schematic shape of domain is shown in figure 3. The dimension of domain has been obtain after doing several various lengths for b, f, u and independent lengths have been chosen. The grid sizing was determined after grid independence that was found by doing several different trials.

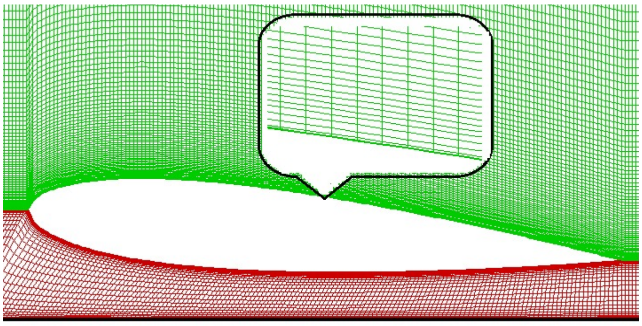

Fig. 2 grid topology and H grid for 2D case

Table II shows 2D grid independent results. For other cases, the above process is used for grid and domain independences.

According to the Figure 3, at the inlet, velocity has been prescribed. At outlet, the pressure is fixed. Slip boundary conditions are used on upper walls of the domain and wall boundary conditions are used for airfoil surface and ground surface.

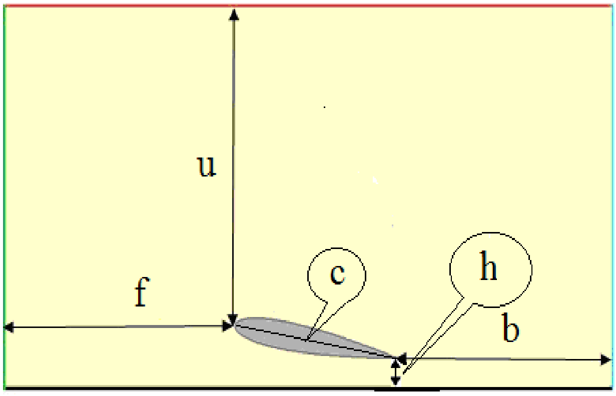

Fig. 3 Dimension of 2D domain

TABLE II
CASES FOR 2D GRID INDEPENDENT

Case name	Number of grid	CL	CD
A	12343 cell	1.2591	0.0340
B	24492 cell	1.2742	0.0311
C	51010 cell	1.2768	0.0299
D	83526 cell	1.2924	0.0281
E	116055 cell	1.2991	0.0286
F	132060 cell	1.3118	0.0428

B. The 3D simulations condition

For 3D cases, Simulation of flow around the wing with AR=2 and airfoil section NACA6409 has been performed. The simulation is three-dimensional, steady stat and flow is incompressible. The Reynolds number for this study is 3.4×10^5.

The 3D grid structure that used is structured mesh cases (see e.g. Figure. 4) except in tip surface zone the unstructured mesh has been used. Schematic figure of 3D computational domain and boundary condition of 3D domain have been shown in Figure 5. According to this figure, at the inlet, velocity has been chosen. At outlet, the pressure is fixed. Slip boundary conditions are applied at upper and left and right boundary. Wall boundary conditions are used for wing surface and ground surface.

In order to find independent grid and domain, various lengths for b, f, u and l has been studied. Also effect of grid sizing has been investigated. The results have been presented in table III. According to these results, case (H) has been chosen for 3D simulation.

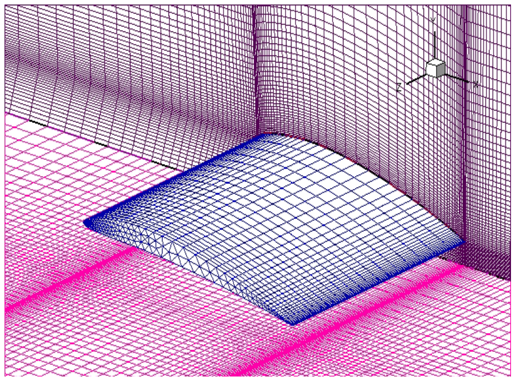

Fig. 4 grid topology and H grid for 3D case

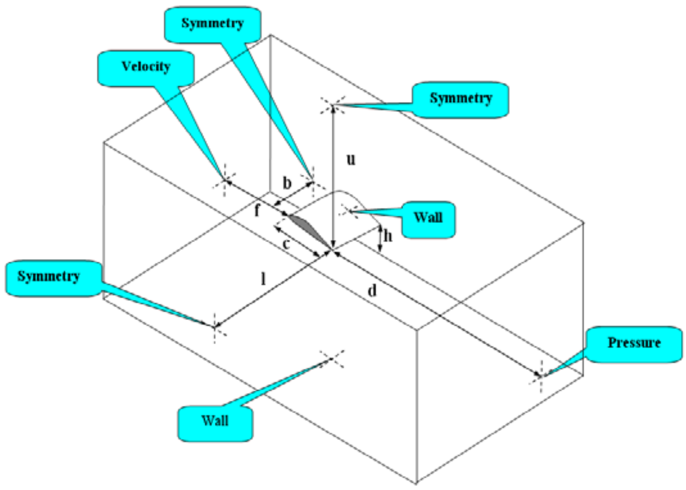

Fig. 5 Dimensions and boundary condition of 3D domain

TABLE III
CASES FOR 3D GRID INDEPENDENT

Case name	Number of grid	Dimensions	CL	CD
A	403800 cell	f=2c, b=6c	1.0097	0.0911

		u=4c, l=2c		
B	433638 cell	f=2c, b=6c u=4c, l=2c	1.0036	0.0900
C	478680 cell	f=3c, b=6c u=4c, l=3c	0.9532	0.0863
D	575055 cell	f=4c, b=6c u=4c, l=4c	0.926	0.0847
E	776350 cell	f=6c,b=10c, u=4c, l=6c	0.8604	0.0795
F	824468 cell	f=2c, b=6c u=4c, l=2c	1.017	0.0924
G	1028828 cell	f=6c,b=10c u=4c, l=6c	0.857	0.0793
H	1028828 cell	f=6c, b=10c u=6c, l=6c	0.861	0.0801

C. Effect of turbulence model

The main emphasis of this paper is the effect of turbulence model to simulation of 3D wing and 2D airfoil in ground proximity and results have been presented in this section.

Figure 6 shows the Lift coefficient of NACA0015 airfoil for different turbulence models at the AOA 5° and different ground clearances. The $k-\omega$ SST model predict lower lift coefficient and $k-\varepsilon$ RNG has different result. Other turbulence models show good results. All experimental data for 2D cases in present research is from publication of ahmed et al. [2].

Figure 7 shows the Drag coefficient of NACA0015 airfoil for different turbulence models at the AOA 5° and different ground clearances. It shows that the $k-\varepsilon$ *RNG* is not in a good agreement with other turbulence models and the Reynolds stress model has better results than others.

Figures 8 shows the velocity profile of wake flow at x/c=0.5 and x/c=1 from trailing edge behind the 2D airfoil NACA0015 at AOA=5° and h/c=0.1. The diagram has compared results of different turbulence model with experimental data. Comparisons show that the RSM and SA model has similar prediction of velocity and more adapted with experimental results.

Figure 9 shows pressure coefficient distribution on the airfoil surfaces for different turbulence models for AOA=5° and h/c=0.1. Comparison of turbulence models indicate that $k-\varepsilon$ RNG model predict higher Cp on the pressure side of the airfoil. Also $k-\omega$ SST model predict lower Cp. This phenomenon is in agreement with the behavior of CL that presented in table IV. Comparison show that the CL of $k-\varepsilon$ RNG is higher than other turbulent model because the different between pressure and suction said of the airfoil is higher. Also the Cp on the pressure said and as results the CL is lower than other turbulence model. Consider that the behavior of CD is not in agreement with pervious discussion. Not that the drag is due to pressure drag and friction drag and the prediction of friction drag lead to different behavior for CD. Figures10 shows pressure coefficient distribution on the airfoil surfaces for different turbulence models at the AOA= 5° and h/c=0.5. The result shows that there is not considerable different for turbulence model for Cp except in the suction side at leading edge.

Comparison of figures 9 and 10 shows that the turbulence models affect on Cp distribution in the lower ground clearance.

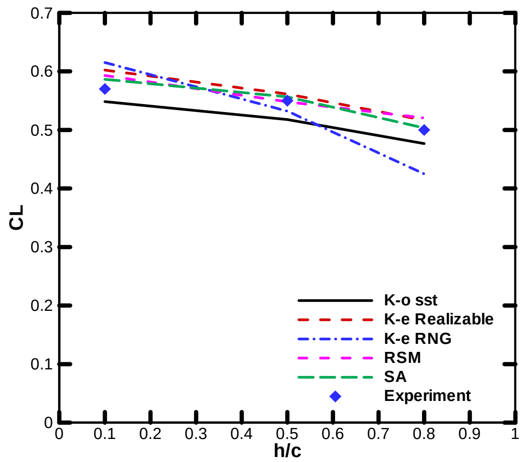

Fig. 6 Lift coefficient of NACA0015 airfoil for different turbulence models at the AOA= 5° and different ground clearances

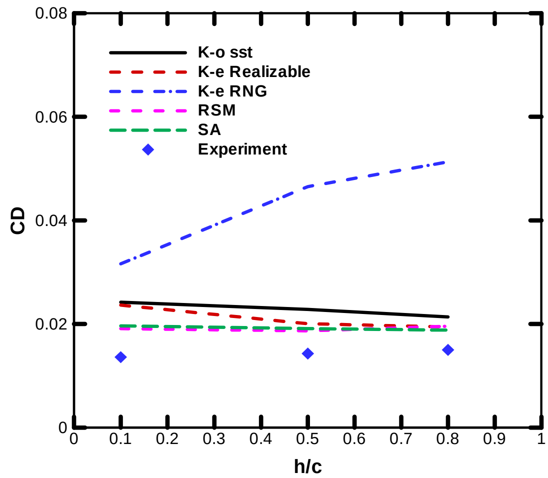

Fig. 7 Drag coefficient of NACA0015 airfoil for different turbulence models at the AOA= 5° and different ground clearances

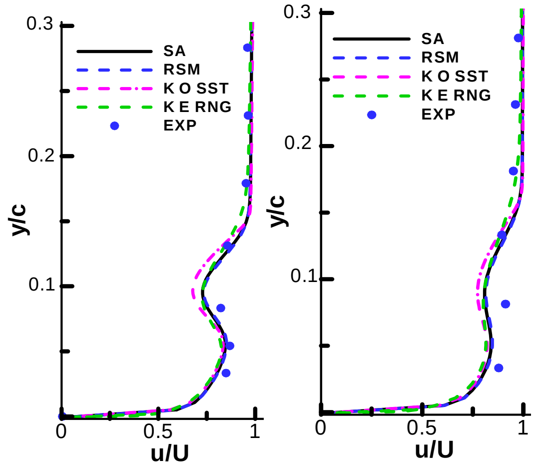

(a) (b)

Fig. 8 velocity profile at (a) x/c=0.5 and (b) x/c=1 from trailing edge AOA= 5° and h/c=0.1.

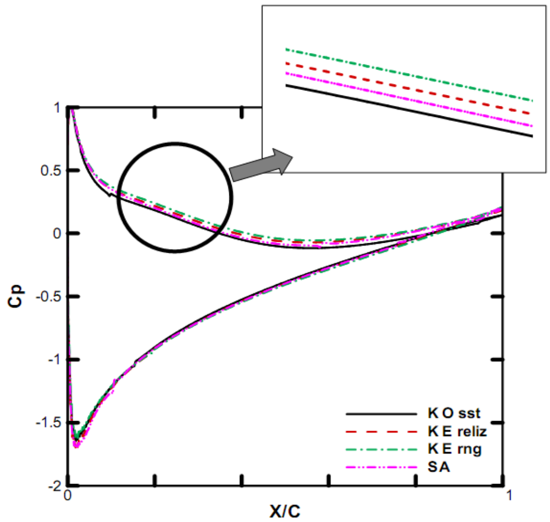

Fig. 9 pressure coefficient distribution on the surface of NACA0015 airfoil for different turbulence models at the AOA= 5° and h/c=0.1

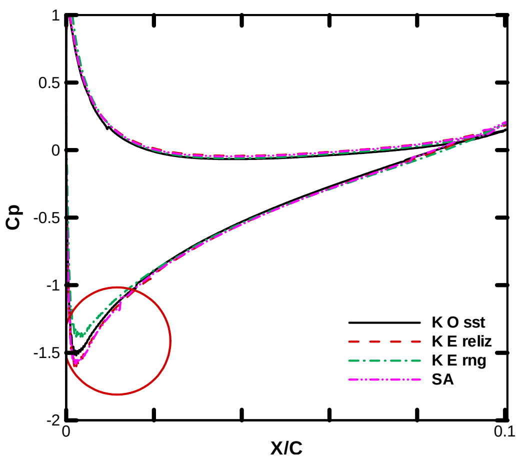

Fig. 10 pressure coefficient distribution on the surface of NACA0015 airfoil for different turbulence models at the AOA= 5° and h/c=0.5

TABLE IV

LIFT AND DRAG COEFFICIENT FOR AOA= 5°

Turbulence models	h/c=0.1		h/c=0.5	
	CL	CD	CL	CD
SA	0.587	0.0196	0.557	0.0191
$k-\varepsilon$ RNG	0.615	0.0316	0.532	0.0465
$k-\varepsilon$ Realizable	0.602	0.0237	0.561	0.0201
RSM	0.593	0.0191	0.548	0.0187
$k-\omega$ SST	0.548	0.0242	0.518	0.0228
Experimental	0.672	0.01360	0.586	0.0143

Figure 11 shows the Lift coefficient of wing for different turbulence model at AOA=8° and different ground clearances. This comparison shows that the $k-\omega$ SST can not predict trend of lift varying in ground effect. Figure 12 shows the drag coefficient of it for different turbulence models at AOA=8° and different ground clearance. It show that the behavior of drag coefficient is in agreement with experimental data for all turbulence models but the SA and RSM model have the lowest different with experimental data. All experimental data for 3D cases in present research is from publication of Jung et.al.[8].

Figure 13(a)-13(d) compares the computed streamlines at AOA=8° and h/c=0.05 for different turbulence model. Comparisons show that the $k-\omega$ SST model has been shown great separation on trilling edge. The RSM and SA model predict small separation on trilling edge. $k-\varepsilon$ RNG model has not show any separation on that zone. Figure 14and 15 compare separation of SA model at trilling edge for h/c=0.3 and h/c=0.05. It can be seen that the separation has not happen for h/c=0.3. It could be said that the separation has been happened in lower ground clearance. Comparisons of figure 13(b) and 15 compare streamlines around a 2D airfoil NACA6409 and root of wing for $k-\omega$ SST turbulence model for h/c=0.05. Consider the zone that marked with circle in figure 15 that show the vortex under the 2D airfoil. Comparisons indicate that in 2D cases vortex has been exist while there is not exist in 3D cases. The reason is that in 2D cases the stronger pressure gradient has been exist in this zone and leads to flow separation and vortex.

Figures 16 shows pressure coefficient distribution on the airfoil surfaces for different turbulence models at AOA=8° and h/c=0.05. It shows various predication of Cp on the surface of airfoil. Consider the zone than marked with circle. This is the zone that the separation has been predicted. These indicate that the various separation patterns on trilling edge lead to different pressure coefficient distribution on this zone. Other considerable phenomena is that the Cp is almost constant in separation zone and equal to separation point pressure. This is in agreement with other published previous researches [18].

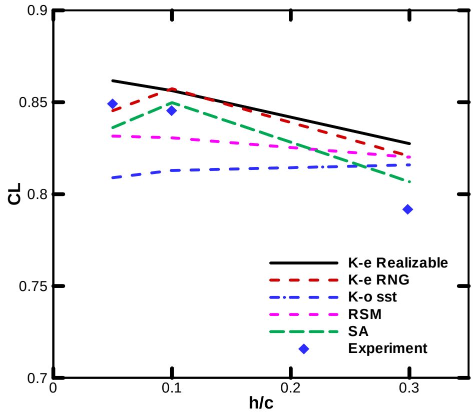

Fig. 11 Drag coefficient of wing with airfoil section NACA6409 for different turbulence models at AOA= 8° and different ground clearance.

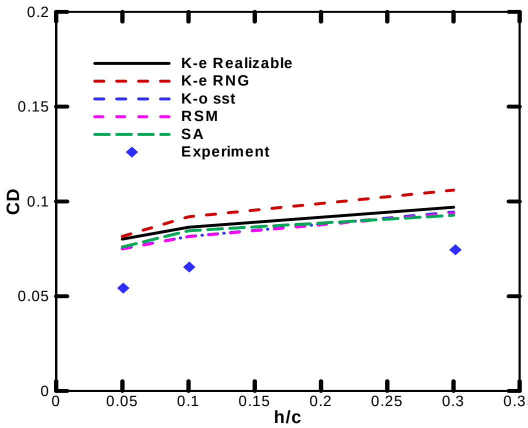

Fig. 12 Drag coefficient of wing with airfoil section NACA6409 for different turbulence models at AOA= 8° and different ground clearance.

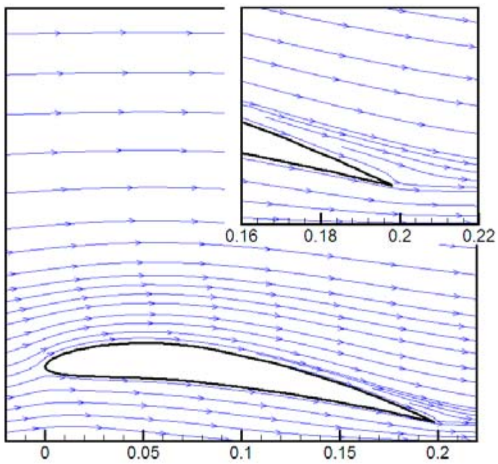

(a)

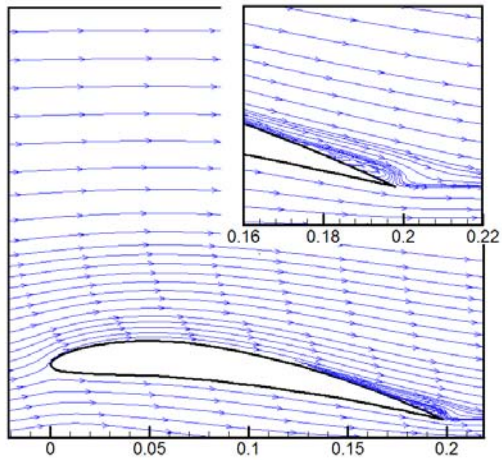

(b)

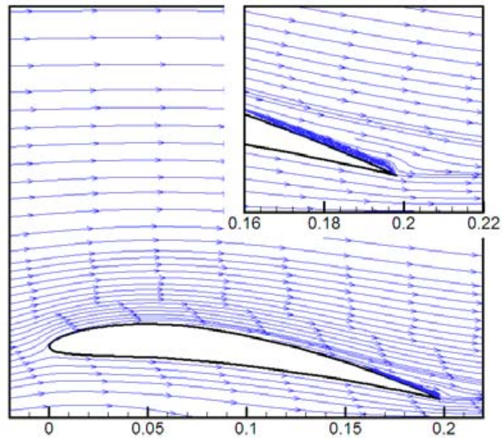

(c)

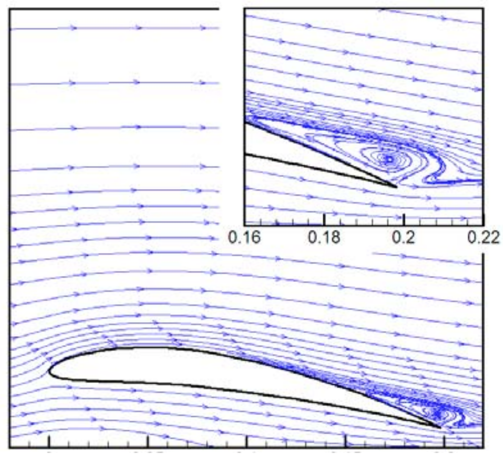

(d)

Fig. 13 Streamlines around the root of wing due to ground proximity for (a) $K-\varepsilon$,(b) SA,(c) RSM,(d) $K-\omega\ SST$ turbulence model for h/c=0.05

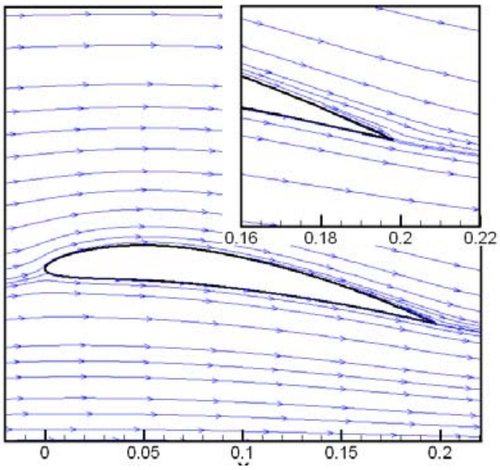

Fig. 14 Streamlines around the root of wing due to ground proximity by SA turbulence model for AOA= 8° and h/c=0.3.

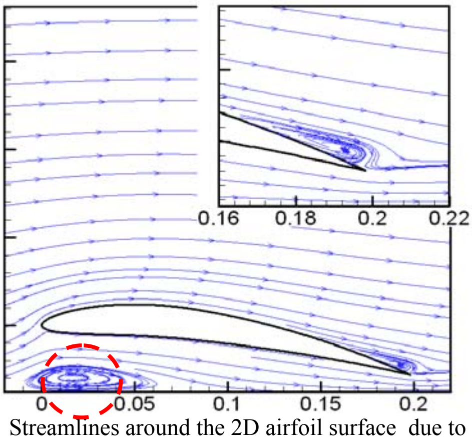

Fig. 15 Streamlines around the 2D airfoil surface due to ground proximity by SA turbulence model for AOA= 8° and h/c=0.05.

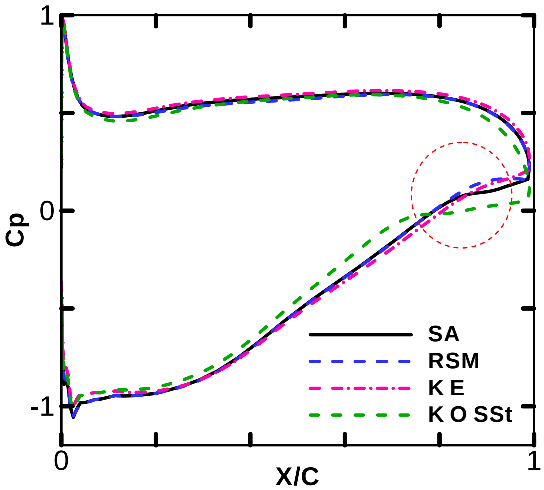

Fig. 16 pressure coefficient distribution on root of wing with NACA6409 airfoil section for different turbulence models at the AOA= 8° and h/c=0.05

IV. Conclusion

1- In present research the effect of turbulence models on simulation of 2D airfoil and 3D wing in the ground effect has been carried out.

2- For 2D simulation the results of RSM and SA model is more adapted with each other and experimental data.

3- Also for 3D simulation the results of RSM and SA model is more adapted with each other and experimental data.

4- The $k-\omega$ SST predicts more separation in ground effect.

5- The separation is increases in lower ground clearance.

Finally the result shows that Spalart-Allmarast is interested for 2D and 3D cases because of its simplification, lower computational cost and its good agreement with experimental results.

References

[1] M.R. Ahmed,., and S. D. Sharma, "Experimental investigation of the flow field of a symmetrical airfoil in ground effect". *21st Applied Aerodynamics Conf*, 2003, Orlando, Florida.

[2] M.R. Ahmed,., and S. D. Sharma, "An investigation on the aerodynamics of a symmetrical airfoil in ground effect", *Experimental Thermal and Fluid Science*, 2005, p: 633–647.

[3] H.Kawazoe, T.Yorikane and Y.Tone., "A study on dynamic characteristics of delta wing in rolling motion near ground". *39th AIAA Aerospace Sciences Meeting & Exhibit,* 2001 Reno, NEVADA.

[4] K. L. Kliment, and K. Rokhsaz, "Experimental Investigation of Pairs of Vortex Filaments in Ground Effect", *36th AIAA Fluid Dynamics Conference and Exhibit,* 2006 San Francisco, California.

[5] X. Zhang and J. Zerihan, "Aerodynamics of a Double Element Wing in Ground Effect", *40th AIAA Aerospace Sciences Meeting and Exhibit*, 2002, Reno, Nevada.

[6] B. L. Jones, M. E. Franke, and E. J. Stephen., "Aerodynamic Ground Effects of a Tailless Chevron-Shaped UCAV Model", *24th Applied Aerodynamics Conference, 2006*, San Francisco, California.

[7] D. J. Ogurek and J. Ashworth, "Experimental Investigation of Various Winglet Designs for a Wing in Ground Effect", *22nd Applied Aerodynamics Conference and Exhibit*, 2004, Providence, Rhode Island.

[8] K. H. Jung , C. Hee., and J. Kim, "Experimental investigation of wing-in-ground effect with a NACA6409 section", 2008,J Mar Sci Technol.

[9] J. L. Smith, H. Z. Graham, and J. E. Smith, "The Validation of an Airfoil in the Ground Effect Regime Using 2-D CFD Analysis", *26th AIAA Aerodynamic Measurement Technology and Ground Testing Conference
*, 2008, Seattle, Washington.

[10] P. Vu,"CFD study of wing tip vortices for inverted airfoils in ground effect", *MS Thesis*, School of engineering, 2006, Cranfield University.

[11] K. Park , and J. Lee, "Influence of endplate on aerodynamic characteristics of low-aspect-ratio wing in ground effect*", Journal of Mechanical Science and Technology* , 2008, 22 2578~2589.

[12] T.Abramowski.," Numerical investigation of airfoil in ground proximity", *Journal of Theoretical and applied Science* 45, 2, 2007, pp. 425-436, Warsaw.

[13] Y.J. Moon, H.J. Oh, and J.H. Seo, "Aerodynamic investigation of three-dimensional wings in ground effect for aero-levitation electric vehicle", *Aerospace Science and Technology* 9, 2005, PP.485–494.

[14] G. M. Angle, B. M. O'Hara, F.A. Pertl, and J. E. Smith, "Pitch Stability Analysis of an Airfoil in Ground Effect*", Journal of Aircraft,* Vol. 46, No. 3, 2009, May–June.

[15] H.J Kim, H. H. Chun, and K. H. Jung, "Aeronumeric optimal design of a wing-in-ground-effect craft", *J Mar Sci Technol*, 2009 DOI 10.1007/s00773-008-0020-7.

[16] P.J. Boschetti, E.M. Cárdenas, and A. Amerio., "Stability and Performance of a Light Unmanned Airplane in Ground Effect", *48th AIAA Aerospace Sciences Meeting Including the New Horizons Forum and Aerospace Exposition*, 2010, Florida.

[17] J. Lee, C.H. Hong, B.S. K.K. Park and J.K. Ahn., "Optimization of Wings in Ground Effect Using Multi- Objective Genetic Algorithm", *48th AIAA Aerospace Sciences Meeting Including the New Horizons Forum and Aerospace Exposition*, 2010, Florida.

[18] F.M. White, "Viscous fluid flow", *McGraw-Hill*, 1991.